Control Engineering Practice 16 (2008) 897–908

Emulator-based control for actuator-based hardware-in-the-loop testing

P.J. Gawthrop [a] D.W. Virden [b] S.A. Neild [b] D.J. Wagg [b,1]

[a] *Centre for Systems and Control and Department of Mechanical Engineering, University of Glasgow, GLASGOW. G12 8QQ Scotland.*

[b] *Department of Mechanical Engineering, Queens Building, University of Bristol, Bristol BS8 1TR, UK.*

Abstract

Hardware-in-the-loop (HWiL) is a form of component testing where hardware components a linked with software models. In order to test mechanical components an additional *transfer system* is required to link the software and hardware subsystems. The transfer system typically comprises of sensors and actuators and the dynamic effects of these components need to be eliminated to give accurate results. In this paper an emulator-based control strategy is presented for actuator based HWiL. Emulator-based control can solve the twin problems of stability and fidelity caused by the unwanted transfer system (actuator) dynamics. Significantly EBC can emulate the inverse of a transfer system which is not causally invertible, allowing a wider range of more complex transfer systems to be controlled. A robustness analysis is given and experimental results presented.

Key words: Hardware-in-the-loop; feedback control; robustness; automotive engineering.

Control Engineering Practice 16 (2008) 897–908

1 Introduction

Hardware-in-the-loop (HWiL) is a form of component testing where physical components of the system communicate with software models which simulate the behaviour of the rest of the system (Brendecke & Kucukay , 2002; Faithfull et al. , 2001; Zhang & Alleyne , 2005). Typically the hardware components being tested are control systems and the method has particular applications in the automotive industry (Hong et al., 2002; Misselhorn et al., 2006; Rulka & Pankiewicz , 2005) and a range of other applications (de Carufel et al., 2000; Ferreira et al., 2004a,b; Ganguli et al., 2005; Jezernik , 2005; Lambrechts et al., 2005; Mansoor et al., 2003). In a typical hardware-in-the-loop test, the hardware component consists of a box of electronic components which can communicate with the software models via electrical signals exchanged using a data acquisition and control system such as dSpace. Extending the HWiL technique to test mechanical components has been an area of interest for some time, for example, for use in suspension development, see (Misselhorn et al., 2006) and references therein. The main difficulty is that connecting a mechanical component to a software model requires the transfer of forces and velocities, and to achieve this an additional dynamic *transfer system* (Wagg & Stoten, 2001) must be included in the loop. Typically the transfer system is a set of actuators, which will have dynamic characteristics which need to be compensated for if the test is to be carried out in real time.

Mitigating the effect of transfer system dynamics has been studied in detail in the

[1] Corresponding author. Email: david.wagg@bristol.ac.uk; Tel. +44 (117) 9289736, Fax: +44 (117) 929 4423

context of the related testing technique of real time dynamic substructuring (RTDS) (Blakeborough et al., 2001; Darby et al., 2002; Gawthrop et al., 2005b; Horiuchi et al., 1999; Reinhorn et al., 2004). The topic of real-time dynamic substructuring is the subject of a recent issue of Philosophical Transactions of the Royal Society, within which Williams & Blakeborough (2001) give an excellent introductory review. Real time dynamic substructuring is an actuator based HWiL technique (Ab-HWiL), which so far has primarily been considered for civil engineering systems. As a result instability is a frequent problem because the systems being modelled usually have lightly damped resonant behaviour, and any small delays in the transfer system have the effect of negative damping (Horiuchi et al., 1999; Wallace et al., 2005a).

The effect of transfer system dynamics can be mitigated by reformulating the problem as a feedback control problem, so that the techniques of robust control design can be applied to ensure stability (Gawthrop et al., 2006), but at the cost of reduced accuracy. In a small number of cases, the dynamics of the transfer system can be removed from the closed loop by using an inverted model of the transfer system dynamics — for example, using the virtual actuator approach (Gawthrop, 2004, 2005; Gawthrop et al., 2005b) — in most cases however, the transfer system is not (causally) invertible. One of the most commonly considered examples of a non-invertible transfer system is that of a pure time delay. A number of approaches have been suggested to compensate for a pure delay including polynomial extrapolation (Darby et al., 2002; Horiuchi & Konno, 2001; Wallace et al., 2005a,b), adaptive forward prediction (Darby et al., 2002; Wallace et al., 2005b,b) and Smith's predictor (Agrawal & Yang, 2000; McGreevy et al., 1998; Reinhorn et al., 2004).

In the automotive suspension systems studied by (Misselhorn et al., 2006) the damping levels are significantly higher than in most RTDS tests, such that phase margin instabilities can be avoided. In fact the approach is to use PID control, and operate in a frequency range where actuator phase lag is seen to be acceptable. However, for mechanical components with lower damping, we believe that the delay compensation techniques developed for RTDS will be of significant benefit for actuator based HWiL. This will also apply to applications where electro-mechanical devices or complex circuitry are used as transfer systems, with the result that the effect of their dynamics may be significant (Driscoll et al., 2005; Zhu et al., 2005). It will also be useful for the development and techniques such as model-in-the-loop (Plummer , 2006; Zhu et al., 2005) and engine-in-the-loop (Fathy et al., 2006) testing which are further extensions of the HWiL technique.

In this paper, we propose the use of the emulator-based control strategy for actuator based HWiL. Emulator-based control (EBC) gives a novel and effective solution to the twin problems of stability and fidelity caused by the unwanted transfer system (actuator) dynamics. In particular EBC can emulate the inverse of a transfer system which is not causally invertible. Moreover, the approach can be used with more complex models of transfer system dynamics than have previously been studied. This means that more accurate coupling can be obtained, leading in turn to a higher degree of accuracy for the complete test. This will be demonstrated using an example of the lightly damped mass-spring-damper system previously considered in (Wallace et al., 2005b).

2 Actuator based HWiL as a feedback system

This section shows that the actuator-based HWiL (AbHWiL) approach introduced in this paper has a feedback interpretation and that standard frequency domain results (for example as discussed in the textbook of Goodwin et al. (2001)) can be used to analyse the resultant feedback loop.

AbHWiL involves having a model in two parts, one to be tested as a hardware component and one to be implemented as a software model. In this paper, the analysis is accomplished in the continuous-time domain thus regarding not only the tested component but also the software component as a physical system. The implementation of the software component (including choice of integration method and sample time) is an important issue which is not, however, covered in this paper.

Because the complete system being modelled is a physical system, each of the two subsystems has the special mathematical property of passivity (Willems, 1972) which can be expressed in bond graph terms (Gawthrop et al., 2005b). The software subsystem is connected to the hardware subsystem via a computer digital to analogue interface driving a physical actuator; the connection is referred to as the transfer system.

[Fig. 1 about here.]

Gawthrop et al. (2006) showed how RTDS (and hence AbHWiL) can be viewed as a feedback system, represented in conventional block diagram form in figure 1, where $P(s)$ is the transfer function of the hardware component, $N(s)$ and $N_r(s)$ the transfer functions representing the software model (which is driven by the refer-

ence signal $r(s)$ as well as the physical subsystem output $y(s)$) and $T(s)$ the transfer function of the transfer system. For the case where interface displacement is passed from the software model to the hardware component, $u(s)$ is the interface displacement calculated by the software model, $x(s)$ is the displacement imposed on the hardware component, $y(s)$ is the force required to impose the displacement $x(s)$ on the hardware component and $r(s)$ is the external excitation. In the ideal situation, $T(s) = 1$ so that the software model output matches the hardware component input exactly (and hence the AbHWiL system perfectly replicates the full physical system). In this ideal case the closed-loop system of figure 1 has the closed-loop transfer function $\frac{y(s)}{r(s)} = Y(s)N_r(s)$ given by

$$Y(s) = \frac{N(s)P(s)}{1 + N(s)P(s)} \tag{1}$$

For the analysis in this paper the following assumptions are made:

Assumption 1 *$P(s)$ and $N(s)$ are stable rational transfer functions.*

Assumption 2 *$Y(s)$ and $N_r(s)$ are stable.*

Assumption 1 implies that

$$P(s) = \frac{B_P(s)}{A_P(s)} \tag{2}$$

$$N(s) = \frac{B_N(s)}{A_N(s)} \tag{3}$$

where the numerator and denominator of each transfer function is a polynomial in the Laplace operator s. Assumption 2 implies that the complete physical system being tested using the substructuring technique is stable. Define σ_i as the ith root of the polynomial A_{cl} where

$$A_{cl} = A_N(s)A_P(s) + B_N(s)B_P(s) \tag{4}$$

so that assumptions 1 and 2 imply $\Re\sigma_i < 0 \forall i$.

As illustrated in §44.2 and §55.3 the feedback system of figure 1 typically has a very poor stability margin (in a sense to be defined later); thus the problem of achieving stability and fidelity when $T(s) \neq 1$ is not trivial; this paper shows that EBC can solve this problem in a novel way.

3 Emulator-based Control

Smith's predictor (Marshall, 1979; Smith, 1959) is an example of a controller using a built-in mathematical model of the controlled system. Although the technique was developed in the process industry to overcome problems in controlling time-delay systems, it has been suggested (Agrawal & Yang, 2000; McGreevy et al., 1998; Reinhorn et al., 2004) as method of overcoming time delay in transfer systems. Unfortunately, Smith's predictor has serious limitations for AbHWiL/RTDS. In particular, it has poor performance when the controlled system is lightly-damped. Research on an alternative form of predictive control, based on stochastic time series analysis – initiated by Åström (1970) – lead to the development of (discrete-time) self-tuning control (Åström & Wittenmark, 1973; Clarke & Gawthrop, 1975). Continuous-time versions of self-tuning controllers (and associated predictors) were developed by Gawthrop (1987) and lead to the *emulator-based control* (EBC) approach (Gawthrop et al., 1996) which overcomes the limitations of Smith's predictor mentioned above.

[Fig. 2 about here.]

Figure 2(a) gives the basic idea of emulator based control (Gawthrop, 1987; Gawthrop et al., 1996). The controlled system is represented by a rational transfer function $\frac{B(s)}{A(s)}$ combined with the pure time delay of τ represented by the transfer function $e^{-s\tau}$; the system input (control signal) is $u(s)$ and system output is $y(s)$. The transfer function $\frac{C(s)}{A(s)}$ and the signal $\xi(s)$ represent the combined effect of all disturbances and measurement noise affecting the system.

To control this system it is desirable to modify the closed loop response by applying the transfer function $e^{s\tau}\frac{\mathbb{P}(s)}{B^-(s)}$ to the feedback signal, as shown in figure 2(a), where $B^-(s)$ contains the all of the roots of $B(s)$ with positive real parts[2] and $\mathbb{P}(s)$ is a *design parameter*. However this transfer function is unrealisable. The general EBC strategy (Gawthrop, 1987; Gawthrop et al., 1996) focuses on the *unrealisable* transfer function $e^{s\tau}\frac{\mathbb{P}(s)}{B^-(s)}$ of figure 2(a); this transfer function is unrealisable for some, or all, of the following reasons:

(1) When $\tau > 0$, $e^{s\tau}$ represents a pure prediction.
(2) When the real part of at least one root of $B^-(s)$ is positive, the system represented by $\frac{1}{B^-(s)}$ is non-causal.
(3) If degree of $\mathbb{P}(s) >$ degree of $B^-(s)$, $\frac{\mathbb{P}(s)}{B^-(s)}$ is improper.

In the general EBC strategy, as well as $\mathbb{P}(s)$, three further *design parameters* may be used; $\mathbb{R}(s)$, $\mathbb{Q}(s)$ and $C(s)$ (Gawthrop et al., 1996).

[2] One possibility is $B^-(s) = B(s)$, another is to factorise $B(s) = B^-(s)B^+(s)$ where $B^-(s)$ contains only the roots with positive real part and $B^+(s)$ contains only the roots with negative real part

In this paper, this general formulation is replaced by the particular formulation where the *unrealisable* transfer function $e^{s\tau}\frac{\mathbb{P}(s)}{B^{-}(s)}$ is identified with inverse transfer system $T(s)^{-1}$. This allows for a transfer system which may contain a pure delay, zeros with positive real parts and more poles than zeros to be, in effect, removed from the closed-loop feedback system.

In both the general and particular cases, the unrealisable transfer function is replaced by the (realisable) *emulator*. This replacement has two consequences; an exogenous error $e^{\star}(s)$ is introduced (as shown in the feedback loop in figure2(a)) and the sensitivity of the closed-loop system to modelling error is changed. Both of these consequences are affected by the choice of the polynomial $C(s)$, which appears in the emulator formulation. In fact, as discussed later, there are a number of interpretations to be placed on $C(s)$. For the purposes of this paper, it will be regarded as a *design parameter* to be chosen as part of the control system design.

The key finding reported in this paper is that the standard EBC strategy can be modified for AbHWiL. For the AbHWiL application the following assumption is made:

Assumption 3 *$T(s)$ is a stable transfer function.*

As discussed previously (Gawthrop et al., 2006), we believe that the transfer system transfer function $T(s)$ should comprise well-designed hardware and control algorithms, so Assumption 3 is reasonable. Following the notation of Gawthrop et al. (2006), the transfer system is represented by the *stable* transfer function

$$T(s) = e^{-s\tau}\frac{B_T(s)}{A_T(s)} \tag{5}$$

The proposed EBC AbHWiL strategy is shown in figure 2(b). To achieve this control structure the following equivalence between figures 2(a) and 2(b) is used:

$$e^{-s\tau}\frac{B(s)}{A(s)} = T(s)P(s) = \left(e^{-s\tau}\frac{B_T(s)}{A_T(s)}\right)\left(\frac{B_P(s)}{A_P(s)}\right) \tag{6}$$

$$e^{s\tau}\mathbb{P}(s) = \frac{1}{T(s)} = e^{s\tau}\frac{A_T(s)}{B_T(s)} \tag{7}$$

$$\frac{1}{\mathbb{Q}(s)} = N(s) = \frac{B_N(s)}{A_N(s)} \tag{8}$$

$$\mathbb{R}(s) = N_r(s) \tag{9}$$

It can be seen that if the transfer function $T(s)^{-1}$ was achievable (such that $e^{\star}(s) = 0$) and there is no noise ($\xi(s) = 0$), the dynamics between the software model output $u(s)$ and the feedback to the software model, now represented by $\phi^{\star}(s)$, reduces to the hardware component dynamics $P(s)$ as desired. Compared to the ideal case where there are no transfer system dynamics, $T(s) = 1$, the system output $y(s)$ is however modified by $T(s)$, but this can easily be rectified by prefiltering $r(s)$ by $T(s)^{-1}$ off-line. In the proposed AbHWiL version of the EBC strategy three of the four *design parameters*, $\mathbb{P}(s)$, $\mathbb{R}(s)$ and $\mathbb{Q}(s)$, are determined by the software model and the transfer system dynamics. The fourth design parameter, $C(s)$, which (as will be shown later) appears in the realisable implementation of the emulator, remains user-selectable.

As the inverse transfer system $T(s)^{-1}$ is not realisable, it must be *emulated*; the practical implementation of the emulator given in figure 2(c) is now derived. From figure 2(b)

$$\phi(s) = P(s)u(s) + \frac{1}{T(s)}\frac{C(s)}{A(s)}\xi(s) \tag{10}$$

$$= \frac{B_P(s)}{A_P(s)}u(s) + e^{s\tau}\frac{C(s)}{B_T(s)A_P(s)}\xi(s) \tag{11}$$

noting that from equation 6, $A(s)$ may be rewritten as

$$A(s) = A_T(s)A_P(s) \tag{12}$$

Following previous work (Gawthrop, 1987; Gawthrop et al., 1996), the following *realisability decomposition* is defined:

$$e^{s\tau}\frac{C(s)}{B_T(s)A_P(s)} = e^{s\tau}\frac{E(s)}{B_T(s)} + \frac{H(s)}{A_P(s)} \tag{13}$$

The ideal emulator output $\phi(s)$ is now split into a realisable (causal) emulator output and an error

$$\phi(s) = \phi^\star(s) + e^\star(s) \tag{14}$$

where using equation (13), $\phi^\star(s)$ and $e^\star(s)$ can be written as:

$$\phi^\star(s) = P(s)u(s) + \frac{H(s)}{A_P(s)}\xi(s) \tag{15}$$

$$e^\star(s) = e^{s\tau}\frac{E(s)}{B_T(s)}\xi(s) \tag{16}$$

However, direct access to the noise signal $\xi(s)$ is not available so the equation for $\phi^\star(s)$ must be rearranged using the following relationship (from figure 2(b)):

$$\xi(s) = \frac{A(s)}{C(s)}\left[y(s) - T(s)P(s)u(s)\right] \tag{17}$$

Substituting (17) into (15) and using (13) gives a *realisable* expression for $\phi^\star(s)$:

$$\phi^\star(s) = \frac{F(s)}{C(s)}y(s) + \frac{G(s)}{C(s)}u(s) \tag{18}$$

where:

$$F(s) = A_T(s)H(s) \tag{19}$$

$$G(s) = B_P(s)E(s) \tag{20}$$

Equation (18) is depicted in figure 2(c) together with the AbHWiL system and transfer system.

A key factor in choosing the realisable emulator output given by equation 15 is that the resulting *emulator error*, $e^\star(s)$, (equation 16) does *not* depend on the control signal $u(s)$. It follows that figures 2(b) and 2(c) are equivalent for the purposes of stability – in particular *the transfer system $T(s)$ has been removed from the closed loop* by the use of the emulator equation (18).

To compute the transfer functions appearing in the emulator equations (18),(19) and (20), the realisability decomposition (13) must be solved. This is done for three special cases. Firstly, however, we note that as with the standard EBC formulation certain *design rules* are applied in determining $C(s)$:

Design rule 1 *All roots of the polynomial $C(s)$ give strictly negative real parts.*

Design rule 2 *The degree of the polynomial $C(s)$ is one less than the degree of $A(s)$.*

As we shall see, Design Rule 1 ensures a stable emulator and Design Rule 2 makes sure that the system output is not differentiated by the emulator. In the case of noisy measurements, Design Rule 2 can be replaced by:

Design rule 3 *The degree of the polynomial $C(s)$ is equal to the degree of $A(s)$.*

Design Rule 3 ensures that the system output is low-pass filtered by the emulator.

This general result is now illustrated by some important special cases.

3.1 All-pole transfer system: $T(s) = \frac{1}{A_T(s)}$

In this case, the realisability decomposition (13) becomes:

$$\frac{C(s)}{A_P(s)} = E(s) + \frac{H(s)}{A_P(s)} \tag{21}$$

Equation (21) corresponds to *polynomial long-division* (Gawthrop, 1987) where $E(s)$ is the quotient and $H(s)$ the remainder.

3.2 All-pass transfer system: $T(s) = \frac{B_T(s)}{A_T(s)}$

In this case, the realisability decomposition (13) becomes:

$$\frac{C(s)}{B_T(s)A_P(s)} = \frac{E(s)}{B_T(s)} + \frac{H(s)}{A_P(s)} \tag{22}$$

Equation can be rewritten as:

$$C(s) = E(s)A_P(s) + H(s)B_T(s) \tag{23}$$

Equation (23) is variously known as a *Diophantine equation* or the *Bezout* identity. It can be solved (for $E(s)$ and $H(s)$) using the Euclidean algorithm (MacLane & Birkhoff, 1967) if and only if the greatest common factor of $A_P(s)$ and $B_T(s)$ is also a factor of $C(s)$; typically $A_P(s)$ and $B_T(s)$ have no common factors and so solvability is not usually an issue.

In this case, the realisability decomposition (13) becomes:

$$e^{s\tau}\frac{C(s)}{A_P(s)} = e^{s\tau}E(s) + \frac{H(s)}{A_P(s)} \tag{24}$$

In this case, $E(s)$ is a transcendental transfer function which can, however, be approximated by rational transfer function; $H(s)$ is a polynomial in s. An example appears in §55.2 .

4 Analysis

There are many approaches to the analysis of linear feedback systems (Goodwin et al., 2001). The approach taken here is two-fold: firstly, the *nominal* closed loop system is derived and secondly the robustness of this nominal system to perturbations in the various transfer functions is analysed in the frequency domain.

4.1 Nominal closed-loop system

From figure 2(b), the closed-loop system can be written as:

$$y(s) = \frac{N(s)P(s)}{1+N(s)P(s)}T(s)(N_r(s)r(s)+e^\star(s)) + \frac{1}{1+N(s)P(s)}\frac{C(s)}{A(s)}\xi(s) \tag{25}$$

$$= \frac{B_N(s)B_P(s)}{A_N(s)A_P(s)+B_N(s)B_P(s)}T(s)(N_r(s)r(s)+e^\star(s)) + \frac{C(s)A_N(s)}{A_N(s)A_P(s)+B_N(s)B_P(s)}\frac{1}{A_T(s)}\xi(s) \tag{26}$$

Comparing (26) with (1) and considering the special case where $\xi(s) = 0$

$$y(s) = Y(s)T(s)N_r(s)r(s) \tag{27}$$

From assumptions 2 and 3, the system of (27) is stable.

Equation (26) is different in two ways from the ideal closed loop system corresponding to $T(s) = 1$: The factor $T(s)$ occurs in the numerator of the first term of (26) and the emulator error $e^\star(s)$ appears. From (16), $e^\star(s)$ depends only on $\xi(s)$ and does not affect stability; $T(s)$ appears only in the numerator and therefore (from assumption 3 also does not cause instability.

For the purposes of comparison with earlier work (Wallace et al., 2005b), and with reference to figure 2, it is useful to define the ideal transfer function $X(s)$ relating the reference signal $r(s)$ to the transfer system output $x(s)$ when the noise $\xi(s) = 0$. In particular

$$x(s) = X(s)T(s)r(s) \tag{28}$$

$$X(s) = \frac{N(s)N_r(s)}{1 + N(s)P(s)} \tag{29}$$

Equations (28) and (29) are used in §5 5.4 to analyse the experimental results.

As discussed in §2, to obtain correct AbHWiL results, $T(s)$ must be removed from (28). In most cases, the experimental reference signal $r'(s)$ is known in full (either in the time or frequency domain) *before* an AbHWiL test. It is therefore possible to perform non-causal operations (such as a forward time-shift) on $r'(s)$ prior to the experiment. Hence it is assumed in the following that:

$$r(s) = T^{-1}r'(s) \tag{30}$$

[Fig. 3 about here.]

[Fig. 4 about here.]

The nominal system of figure 2(b) has a loop-gain of

$$L_0(s) = N(s)P(s) = \frac{B_N(s)B_P(s)}{A_N(s)A_P(s)} \tag{31}$$

To examine the fundamental issues relating to (31), consider the AbHWiL system of figure 3. It is natural to apply a displacement to a spring, so, in the the context of this paper $y(s) = F_P$ (the measured force) and $u(s) = v_N$ (the applied velocity):

$$P(s) = \frac{k_s}{s} \tag{32}$$

$$N(s) = \frac{s}{ms^2 + cs + k} \tag{33}$$

The corresponding Nyquist diagram appears in figure 4 for three values of damping constant c. It is a fundamental result that connecting two passive systems by energy ports yields a stable system, so it is unsurprising that as revealed by figure 4 the loop-gain has a positive phase margin for each value of c. The numerical values of the phase-margin θ_m appears in table 1 for each value of c.

However, and this is the key point, the phase-margin is *very small* for small values of c. Again, this is unsurprising as this small phase margin is precisely what is required to give a sharp resonance in the overall AbHWiL system of figure 3. This small phase margin gives rise to the extreme sensitivity problem discussed elsewhere (Gawthrop et al., 2005b, 2006; Wallace et al., 2005b); in particular, a small value of c together with neglected dynamics in the transfer system results in

instability. As discussed by Gawthrop et al. (2006), robust stability can be obtained at the expense of fidelity by appropriate control design. However, the main thrust of this paper is to remove the transfer system as accurately as possible thus giving accurate fidelity despite the small phase margin. Nevertheless, the issue of robustness is still crucial and so is analysed further here in the context of EBC.

4.3 Robustness

As mentioned in §3, the fact that the nominal system of figure 2(b) is replaced by the emulator-based system of figure 2(c) means that the analysis is different. In particular, the expression for the loop-gain is no longer given by (31). The actual loop gain is now derived. With reference to figure 2(c), the transfer function $N_a(s)$ of the *augmented software subsystem* relating $y(s)$ to $-u(s)$ is:

$$N_a(s) = -\frac{y(s)}{u(s)} = \frac{N(s)}{1+N(s)\frac{G(s)}{C(s)}}\frac{F(s)}{C(s)} = \frac{B_N(s)F(s)}{A_N(s)C(s)+B_N(s)G(s)} \tag{34}$$

For analysis purposes the following assumption is required:

Assumption 4 *$N_a(s)$ is stable.*

It is part of the EBC design process to ensure that assumption 4 holds. The loop gain $L(s)$ corresponding to figure 2(c) is thus:

$$L(s) = N_a(s)T(s)P(s) = e^{-s\tau}\frac{B_T(s)B_N(s)B_P(s)H(s)}{A_P(s)(A_N(s)C(s)+B_N(s)B_P(s)E(s))} \tag{35}$$

Equation (35) is now used to investigate the robustness of the EBC to errors in modelling the physical system $P(s)$.

[Fig. 5 about here.]

The hardware component of the AbHWiL system has, thus far, been taken to be a known linear system with transfer function $P(s)$. However, such a model may not be accurate and thus it is important to investigate the *robustness* of the EBC approach in the presence of such inaccuracy. To do this, assume that the physical system comprises the nominal system $P(s)$ in series with a *neglected* system $\tilde{P}$. Two stability theorems are given: one for linear time invariant $\tilde{P}$ and one for memoryless nonlinearities.

Theorem 1 *Given assumptions 1– 4, if $\tilde{P}$ is a stable, linear, time-invariant system with transfer function $\tilde{P}(s)$ and if the frequency locus $\tilde{P}(s)L(s)$ does not encircle the -1 point in the complex plane as s traverses the Nyquist D contour, then the perturbed closed-loop system is stable.*

PROOF. This is a restatement of Nyquist's theorem (Goodwin et al., 2001; Nyquist, 1932) for stable open-loop systems. □

Theorem 2 *Given assumptions 1– 4, if $\tilde{P} = \tilde{P}(z)$ is a memoryless, sector-bounded non-linearity where for some $\alpha > 0$*

$$1 - \alpha < \frac{\tilde{P}(z)}{z} < 1 + \alpha \qquad \forall z \neq 0 \tag{36}$$

and if the frequency locus $L(s)$ does not encircle the -1 point in the complex plane as s traverses the Nyquist D contour and the locus does not intersect the circle in the complex plane centred at $\frac{1}{1-\alpha^2}$ with radius $\frac{\alpha}{1-\alpha^2}$, then the system is uniformly asymptotically stable.

PROOF. This is a restatement of the circle theorem of Zames (1966a,b). □

In addition to stability, it would be interesting to obtain bounds on the error caused by such nonlinearities; this is a matter for future research.

5 Experimental Investigation

[Fig. 6 about here.]

The AbHWiL system of figure 3 was experimentally investigated in four stages: identification of the transfer system transfer function $T(s)$, design of the corresponding EBC, robustness analysis and experimental results.

The experimental setup of figure 6 consists of a spring - the hardware component - connected, via a load cell, to an electro-mechanical ball-screw actuator. This actuator is driven by a proprietary controller; in proportional displacement control. In RTDS literature the proprietary controller is often referred to as the *inner-loop* controller to distinguish it from the *outer-loop* control strategy; the EBC in the implementation considered here. The transfer system, $T(s)$, consists of both the inner-loop controller and the actuator. Since the EBC strategy operates in velocity control and the inner-loop controller operates in displacement control the EBC control signal is integrated before being sent as the demand signal to the inner-loop controller. The software model, along with the EBC strategy was written in Matlab-Simulink and run in real-time using a dSpace DS1104 R&D Controller Board.

5.1 Transfer system identification

The response of the transfer system $T(s)$ was measured experimentally by applying a square wave displacement setpoint to the transfer system controller; and the corresponding displacement was measured. The second order with delay model of the form $\hat{T}(s) = e^{-s\tau}\frac{k_t}{m_t s^2+c_t s+k_t}$ was used; this is a special case of (5) where $B_T(s) = 1$. Using an optimisation approach (Gawthrop, 2000; Ljung, 1999), the parameters in Table 2 were found to give a good fit.

5.2 Emulator design

It is convenient to work in a normalised time scale with a time unit of 10ms. With these time units, $\tau = 0.5$ and $T(s) = \frac{1}{0.59656s^2+0.51792s+1}$ The hardware component $P(s)$ (32) is first order and so, using (12) the equivalent system has a third order denominator. Using design rule 2 choose $C(s)$ second order; in particular (in this time-scale) choose

$$C = (1+c_e s)^2 \tag{37}$$

In this case (13) becomes $e^{s\tau}\frac{C(s)}{A_P(s)} = e^{s\tau}E(s) + \frac{H(s)}{A_P(s)}$. This gives (Gawthrop, 1987; Gawthrop et al., 1996):

$$E(s) = c_e^2 s + 2c_e + \frac{1-e^{-s\tau}}{s} \tag{38}$$

$$H(s) = 1 \tag{39}$$

As mentioned in §3, (38) has two problems: it contains an irrational term and it contains an implicit cancellation of s. Both can be overcome by *approximating* the exponential function using the second-order Padé approximation (Marshall, 1979,

table 3.1)

$$e^{-s\tau} \approx \frac{1 - \frac{s\tau}{2} + \frac{(s\tau)^2}{12}}{1 + \frac{1}{2}s\tau + \frac{(s\tau)^2}{12}} \tag{40}$$

This approximation is adequate over the frequency range of interest. It follows that:

$$\frac{1 - e^{-s\tau}}{s} \approx \frac{\tau}{1 + \frac{1}{2}s\tau + \frac{(s\tau)^2}{12}} \tag{41}$$

Thus

$$\frac{G(s)}{C(s)} = \frac{E(s)B(s)}{C(s)} \approx k_s \frac{(c_e^2 s + 2c_e)(1 + \frac{1}{2}s\tau + \frac{(s\tau)^2}{12}) + \tau}{(c_e s + 1)^2(1 + \frac{1}{2}s\tau + \frac{(s\tau)^2}{12})} \tag{42}$$

5.3 Robustness analysis

[Fig. 7 about here.]

Figures 7(a)–7(b) show the Nyquist diagrams for three cases of software system damping $c = 15$ and $c = 1$. In each case, the diagram is plotted for choices of the emulator polynomial $C(s)$ (37): $c_e = 1, 0.5, 0.2, 0.01$ and, for comparison, the nominal loop-gain of figure 4. Table 3 gives the corresponding phase and gain margins. Comparing tables 3 and 1 (the case as $c_e \to 0$), it can be seen that increasing c_e *increases* the *phase* margin and thus *increases* robustness to small phase errors in $T(s)$. On the other hand, both figure 7 and table 3 indicate that increasing c_e *decreases* the *gain* margin and thus *decreases* robustness with respect to uncertainty in k_s. In each case, the small stability margins indicate the demanding nature of the experiments reported here.

A number of experiments were conducted using the apparatus of §55.1 , and the EBC designed in §55.2 . These can be divided into two categories, sinusoidal tests where

$$r(s) = A_i \sin(2\pi f_i t + \theta_i) \tag{43}$$

and multi-sine test where

$$r(s) = \sum_{i=1}^{N} A_i \sin(2\pi f_i t + \theta_i) \tag{44}$$

[Fig. 8 about here.]

Sinusoidal tests (43) were carried out for frequencies $f_i = 3,4,5,6,8,9,10$Hz (43), three values of damping c as listed in figure 3, and two values of emulator constant $c_e = 0.2, 0.5$ (37). A signal at $7Hz$ was omitted as the equipment cannot cope with signals near to the resonance at 7.2Hz. In each case, the measured values of $y = F$ (the spring force measured by the load cell), reference signal r, x (measured transfer system displacement) were recorded every msec for about 5sec. For the purposes of computing the properties of the sinusoid, the data was truncated to give an integer number of periods.

Perhaps the most striking result is qualitative; the EBC was stable even at the low damping ($c = 1$). In contrast, it was not possible to stabilise this system below $c = 3$ using the predictive method reported previously (Wallace et al., 2005b).

The relative gain g and phase ϕ of the sinusoidal signals x and r was computed and compared with those computed from $X(s)T(s)$ (28) using the parameter values of figure 3 and table 2. The results are summarised in figure 8 for the largest ($c = 15$)

and smallest ($c = 1$) damping coefficients and for emulator parameter $c_e = 0.2$; the results for $c = 5$ and $c_e = 0.5$ are similar and not shown. In each case, the experimental and theoretical gains are closely matched indicating good fidelity of the EBC; the phases are not in such good agreement. Further experimental investigation revealed that the spring could be more accurately modelled by including structural damping to give the dynamic spring constant $K(s)$

$$K(s) = k_s + c_s s \tag{45}$$

where the estimated damping was $c_s = 3\text{Nsm}^{-1}$ and that this explained some of the phase error. This is an example of a linear $\tilde{P} = 1 + \frac{c_s}{k_s}s$ as discussed in §4.4.3 .

[Fig. 9 about here.]

To demonstrate the behaviour of EBC when using non-sinusoidal signals, a multi-sine reference r was constructed from (44) using the frequencies of figure 8. Figure 9 shows typical 2sec sequences of desired x_0 and actual x displacements for the same controller parameters used in figure 8. The close match between desired and experimental displacements verifies that the method is appropriate to non-sinusoidal reference signals such as a typical earthquake signal.

It was noted that for small values of input (not shown), the experimental response was dominated by a stable limit cycle at a frequency of about 7Hz; this limit cycle disappeared as the signal levels were increased to the values shown in Figure 9. As the measured displacement showed signs of stiction, we suspect the presence of "friction generated limit cycles" (Olsson & Åström, 2001) due to ball-screw friction in the actuator; this requires further investigation.

6 Conclusion

Emulator based control is a well-established controller design method. In this paper we have shown how it can be used to provide a novel but natural way of removing the unwanted transfer system dynamics from an AbHWiL test. In fact this approach gives a significant improvement in control fidelity over previous methods, as we have demonstrated with the example system considered in this paper. The main advantages are; (i) more complex forms of transfer system dynamics can be compensated for, leading to improved fidelity and stability, (ii) the correct gain and phase compensation are applied at any frequency, without the need for adaption, (iii) multi-frequency signals can be dealt with, and (iv) there is a preexisting robustness theory to guide the choice of design parameters. Unlike previous approaches using Smith's predictor, the method presented here is not restricted to stable systems with well-damped resonances — a critical feature for AbHWiL/RTDS systems with lightly damped resonances. In fact emulator based control has a further advantage over Smith's predictor in that it removes unwanted dynamics described by a rational transfer function as well as those described by a pure time-delay.

To achieve these advantages over previous RTDS approaches, we have exploited the fact that for many applications an approximate linear model of the critical component will be available. The emulator based control is then able to cope with the subsequent under-modelled nonlinearities (and other uncertainties) by using robust nonlinear control techniques, as we have demonstrated by application of the circle criterion. For systems without a linear plant model, or with nonlinearities which do not comply with the assumptions made here, the emulator based control approach

would not be appropriate. An area of future research is to use adaptive emulator approach (in fact there is already a large literature containing not only algorithms but adaptive robustness results for emulator based self-tuning controllers) to allow a wider class of nonlinear critical components to be included.

Acknowledgements

Peter Gawthrop is a Visiting Research Fellow at Bristol University. The other authors would like to acknowledge the support of the EPSRC: David Virden is supported by EPSRC grant (GR/R99539/01) and David Wagg via an Advanced Research Fellowship.

References

Åström, K. J. 1970. *Introduction to Stochastic Control Theory*. Academic Press, New York.

Åström,K. J. & Wittenmark,B. 1973. On self-tuning regulators. *Automatica*, 9: 185–199.

Agrawal,A.K. & Yang,J.N. 2000. Compensation of time-delay for control of civil engineering structures. *Earthquake Engng Struc. Dyn.*, 29(1):37–62.

Blakeborough, A., Williams, M.S., Darby, A.P. & Williams, D.M. 2001. The development of real-time substructure testing. *Philosophical Transactions of the Royal Society pt. A*, 359(1869-1891).

Brendecke,T. & Kucukay,F. 2002. Virtual real-time environment for automatic-

transmission control units in the form of hardware-in-the-loop. *Internationa Journal of Vehicle Design*, 28:(84-102).

de Carufel, J., Martin, E. & Piedboeuf, J. C. 2000. Control strategies for hardware-in-the-loop simulation of flexible space robots. *IEE Proceedings-Control Theory and Applications*, 147:569–579.

Clarke,D. W. & Gawthrop, P. J. 1975. Self-tuning controller. *IEE Proceedings Part D: Control Theory and Applications*, 122(9):929–934.

Darby,A.P., Williams,M.S., & Blakeborough, A. 2002. Stability and delay compensation for real-time substructure testing. *ASCE Journal of Engineering Mechanics*, 128:1276–1284.

Driscoll, S.; Huggins, J.D. & Book, W.J. 2005. Electric Motors Coupled to Hydraulic Motors as Actuators for Hydraulic Hardware-in-the-Loop Simulation. *Proceedings of ASME International Mechanical Engineering Congress and Exposition*, paper IMECE2005-82124.

Faithfull, P. T., Ball, R. J. & Jones, R. P. 2001. An investigation into the use of hardware-in-the-loop simulation with a scaled physical prototype as an aid to design. *Journal of Engineering Design*, 12:231–243.

Fathy, H.K.; Ahlawat, R. & Stein, J.L. 2006. Proper Powertrain Modeling for Engine-in-the-Loop Simulation. *Proceedings of the ASME International Engineering Congress and Exposition*, paper IMECE2005-81592.

Ferreira, J. A., Almeida, F. G., Quintas, M. R. & de Oliveira, J. P. E. 2004. Hybrid models for hardware-in-the-loop simulation of hydraulic systems Part 2: experiments. *Proceedings of the Institution of Mechanical Engineers Part I-Journal of Systems and Control Engineering*, 218:475–486.

Ferreira, J. A., Almeida, F. G., Quintas, M. R. & de Oliveira, J. P. E. 2004. Hybrid

models for hardware-in-the-loop simulation of hydraulic systems Part 1: theory. *Proceedings of the Institution of Mechanical Engineers Part I-Journal of Systems and Control Engineering*, 218:465–474.

Ganguli, A., Deraemaeker, A., Horodinca, M. & Preumont, A. 2005. Active damping of chatter in machine toolsdemonstration with a 'hardware-in-the-loop' simulator. *Proceedings of the Institution of Mechanical Engineers Part I-Journal of Systems and Control Engineering*, 219:359–369.

Gawthrop, P. J. 1987. *Continuous-time Self-tuning Control. Vol 1: Design*. Research Studies Press, Engineering control series., Lechworth, England.

Gawthrop,P. J., Jones, R. W., & Sbarbaro, D. G. 1996. Emulator-based control and internal model control: Complementary approaches to robust control design. *Automatica*, 32(8):1223–1227.

Gawthrop., P.J. 2000. Sensitivity bond graphs. *Journal of the Franklin Institute*, 337(7):907–922.

Gawthrop., P.J. 2004. Bond graph based control using virtual actuators. *Proceedings of the Institution of Mechanical Engineers Pt. I: Journal of Systems and Control Engineering*, 218(4):251–268.

Gawthrop, P.J. 2005. Virtual actuators with virtual sensors. *Proceedings of the Institution of Mechanical Engineers Pt. I: Journal of Systems and Control Engineering*, 219(5):371 – 377.

Gawthrop,P.J., Wallace,M.I. & Wagg, D.J. 2005b. Bond-graph based substructuring of dynamical systems. *Earthquake Engng Struc. Dyn.*, 34(6):687–703.

Gawthrop,P.J.,Wallace, M.I., Neild, S.A. & Wagg, D.J. 2006. Robust real-time substructuring techniques for under-damped systems. *Structural Control and Health Monitoring*, xx(xx):xx–xx, (In press).

Control Engineering Practice 16 (2008) 897–908
G.C. Goodwin, S.F. Graebe, & M.E. Salgado. *Control System Design*. Prentice Hall, 2001.

Hong, K. S., Sohn, H. C. & Hedrick, J. K. 2002. Modified skyhook control of semi-active suspensions: A new model, gain scheduling, and hardware-in-the-loop tuning. *Journal of Dynamic Systems Measurement and Control-Transactions of the ASME*, 12400158–167.

Horiuchi,T. & Konno,T. 2001. A new method for compensating actuator delay in real-time hybrid experiments. *Philisophical Transactions of the Royal Society, Pt.A*, 359:1893–1909.

Horiuchi, T., Inoue, M., Konno, T. & Namita, Y. 1999. Real-time hybrid experimental system with actuator delay compensation and its application to a piping system with energy absorber. *Earthquake Engng Struc. Dyn.*, 28:1121–1141.

Jezernik, S. 2005. Hardware-in-the-loop simulation and analysis of magnetic recording of nerve activity. *Journal of Neuroscience Methods*, 142:295–304.

Lambrechts, P., Boerlage, M. & Steinbuch, M. 2005. Trajectory planning and feedforward design for electromechanical motion systems. *Control Engineering Practice*, 13:145–157.

Ljung,L. 1999. *System Identification: Theory for the User*. Information and Systems Science. Prentice-Hall, 2nd edition.

MacLane, S. & Birkhoff, G. 1967. *Algebra*. Macmillan, New York.

Mansoor, S. P., Jones, D. I., Bradley, D. A., Aris, F. C. & Jones, G. R. 2003. Hardware-in-the-loop simulation of a pumped storage hydro station. *International Jornal of Power and Energy Systems*, 23:127–133.

Marshall, J. E. 1979. *Control of Time-delay Systems*. Peter Peregrinus.

McGreevy, S., Soong, T.T. & Reinhorn, A. M. 1998. An experimental study of

time delay compensation in active structural control. In *Proceedings of the 6th International Modal Analysis Conference-IMAC*, volume 1, pages 733–739.

Misselhorn, W. E., Theron, N. J. & Els, P. S. 2006. Investigation of hardware-in-the-loop for use in suspension development. *Vehicle System Dynamics*, 44: 65–81.

Morari, M. & Zafiriou, E. 1989. *Robust Process Control*. Prentice-Hall, Englewood Cliffs.

Nyquist, H. 1932. Regeneration theory. *Bell Syst. Tech. J.*, 11:126–147.

Olsson, H. & Åström, K.J. 2001. Friction generated limit cycles. *Control Systems Technology, IEEE Transactions on*, 9(4):629–636.

Plummer, A. R. 2006. Model-in-the-loop testing. *Proc IMechE Part I-Journal of Systems and Control Engineering*, 220:183–199.

Reinhorn, A.M. , Sivaselvan, M.V., Liang, Z., & Shao, X. 2004. Real-time dynamic hybrid testing of structural systems. In *Thirteenth World Conference on Earthquake Engineering*, Vancouver. Paper No 1644.

Rulka, W. & Pankiewicz, E. 2005. MBS approach to generate equations of motions for HiL-simulations in vehicle dynamics. *Multibody system dynamics*, 14:367–386.

Smith, O. J. M. 1959. A controller to overcome dead-time. *ISA Transactions*, 6(2): 28–33.

Wagg, D.J. & Stoten, D.P. 2001. Substructuring of dynamical systems via the adaptive minimal control approach. *Earthquake Engng Struc. Dyn.*, 30(6):865–877.

Wallace, M.I., Sieber, J., Neild, S.A., Wagg, D.J. & Krauskopf, B. 2005a. A delay differential equation approach to real-time dynamic substructuring. *Earthquake*

Engng Struc. Dyn., 34(15):1817 – 1832.

Wallace, M.I., Wagg, D.J. & Neild, S.A. 2005b. An adaptive polynomial based forward prediction algorithm for multi-actuator real-time dynamic substructuring. *Proceedings of the Royal Society*, 461(2064):3807 – 3826.

Willems, J. C., 1972. Dissipative dynamical systems, part I: General theory, part II: Linear system with quadratic supply rates. *Arch. Rational Mechanics and Analysis*, 45:321–392.

Williams, M.S. & Blakeborough, A. 2001. Laboratory testing of structures under dynamic loads: an introductory review. *Philosophical Transactions of the Royal Society*, 359:1651–1669.

Zames, G. 1966a. On the input-output stability of time-varying nonlinear systems – part I: Conditions derived using concepts of loop gain, conicity and positivity. *IEEE Trans. on Automatic Control*, 11(2):228–238.

Zames, G. 1966b. On the input-output stability of time-varying nonlinear systems – part II: Conditions involving circles in the frequency plane and sector nonlinearities. *IEEE Trans. on Automatic Control*, 11(3):465–476.

Zhang, R. & Alleyne, A. G. 2005. Dynamic emulation using an indirect control input. *Journal of Dynamic Systems Measurement and Control - Transactions of the ASME*, 127:114–124.

Zhu, W. D., Pekarek, S., Jatskevich, J., Wasynczuk, O. & Delisle, D. 2005. A model-in-the-loop interface to emulate source dynamics in a zonal DC distribution system. *IEEE Transactions on Power Electronics*, 20:438–445.

[Table 1 about here.]

[Table 2 about here.]

[Table 3 about here.]

Control Engineering Practice 16 (2008) 897–908

List of Figures

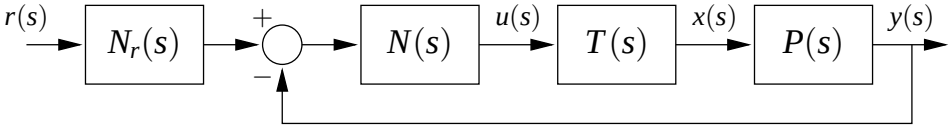

Fig. 1. Substructuring as a feedback system. $P(s)$ is the hardware component transfer function, $N(s)$ and $N_r(s)$ are the software substructure transfer functions and $T(s)$ is the transfer system transfer function.

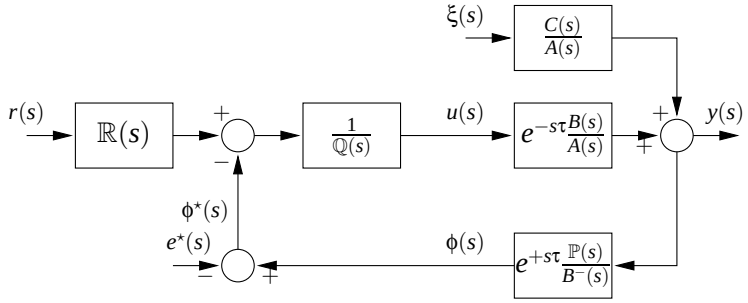

(a) Original formulation

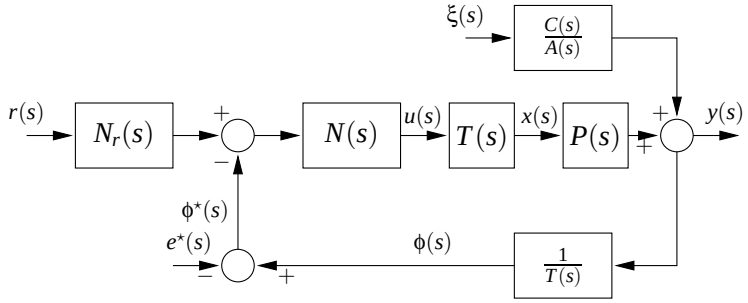

(b) Reformulation for substructuring

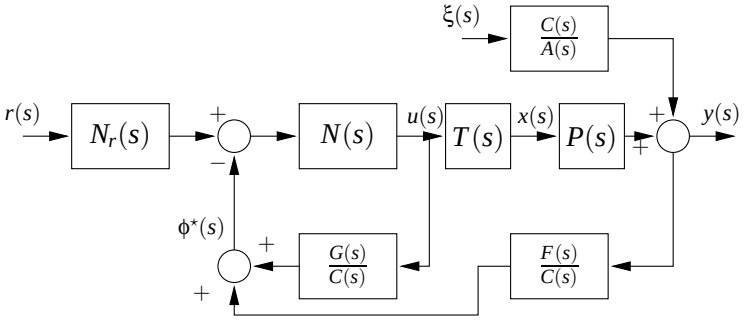

(c) Implementation

Fig. 2. Emulator-based control. (a) shows the general EBC formulation of Gawthrop (1987). (b) shows the particular form appropriate to substructuring which appears to cancel $T(s)$. (c) shows the approximate, but realisable, implementation of (b).

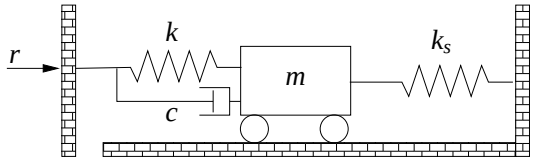

Fig. 3. An AbHWiL system. The physical system, comprising a mass, two springs and a damper, is configured so that the spring k_s is the hardware component; the other components form the software subsystem. r is the imposed wall displacement. The numerical values used are: $c = 1,3$ or $15\text{Nm}^{-1}\text{s}$, $k = k_s = 2250\text{Nm}^{-1}$ and $m = 2.2\text{kg}$

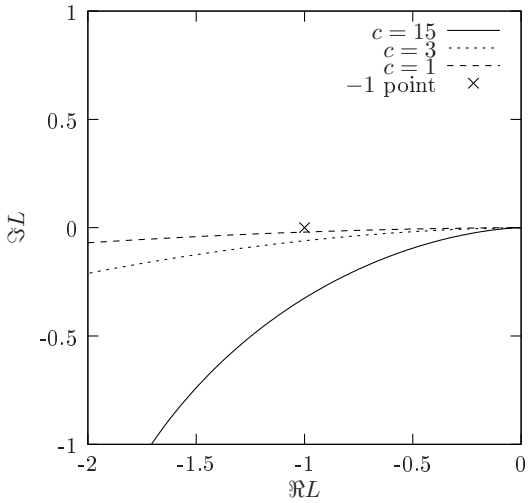

Fig. 4. Nominal loop gain. $L_0(s)$ (31) is plotted for three values of damping coefficient: $c = 15, 3, 1$

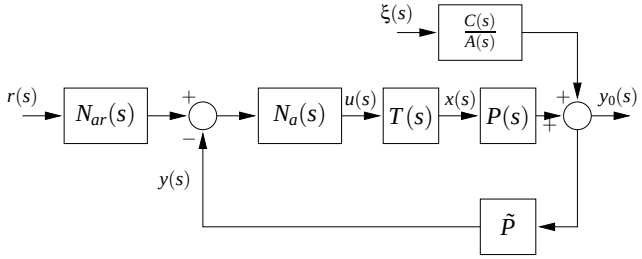

Fig. 5. Robustness analysis. The physical system has been split into a nominal part $P(s)$ and neglected part $\tilde{P}$

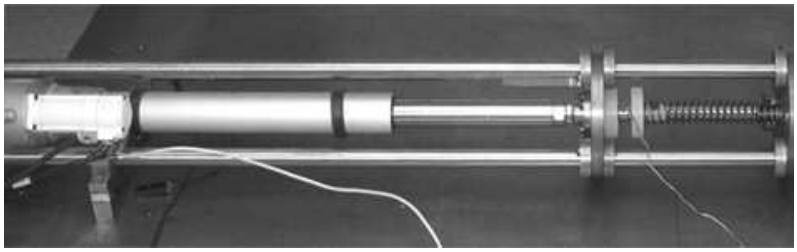

Fig. 6. Experimental Equipment. The hardware component (spring) lies to the right, the transfer system (actuator) is the linear electro-mechanical transducer at the left.

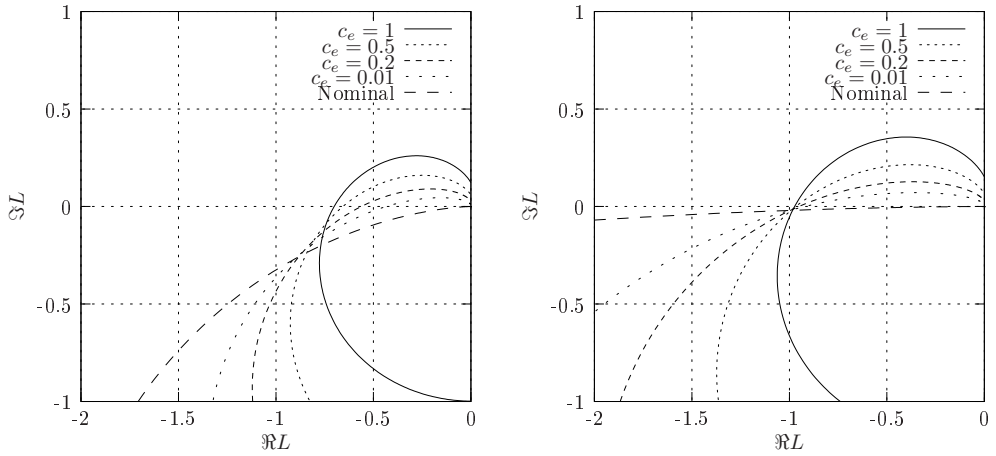

(a) $c = 15$ (b) $c = 1$

Fig. 7. Actual loop-gain. (a) $L(s)$ (35), with damping coefficient $c = 15$, is plotted for five values of damping coefficient: $c_e = 1, 0.5, 0.2, 0.01$ and $c = 1$ as well as for the nominal loop gain $L_0(s)$ (31) of figure 4. (b) is as (a) except that the damping coefficient $c = 1$; the stability margins are smaller in this case.

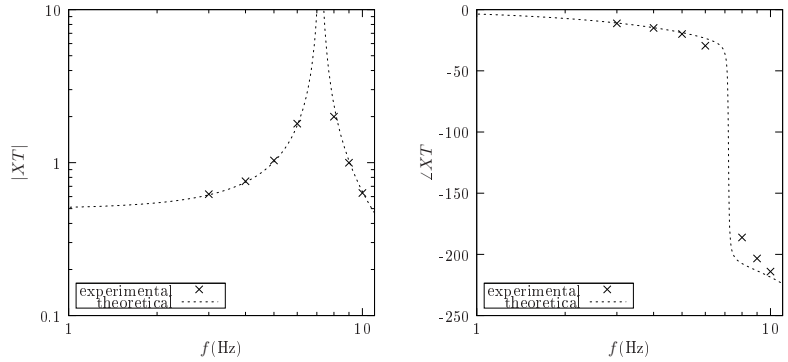

(a) Gain: $c = 1$ (b) Phase: (degrees) $c = 1$

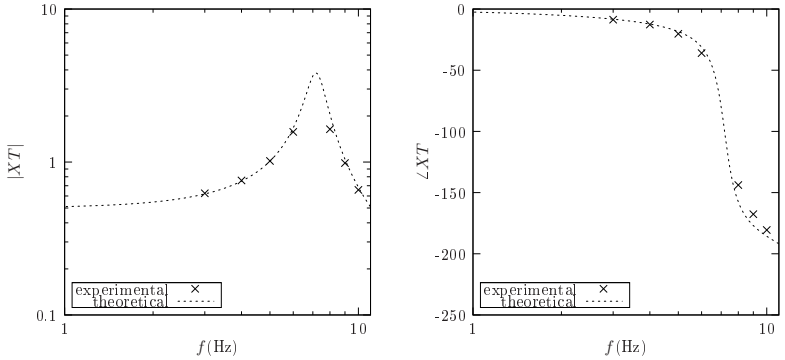

(c) Gain: $c = 15$ (d) Phase (degrees): $c = 15$

Fig. 8. Frequency response. Experimental points marked with $\times$ are superimposed on theoretical frequency response of $T(s)X(s)$ (28).

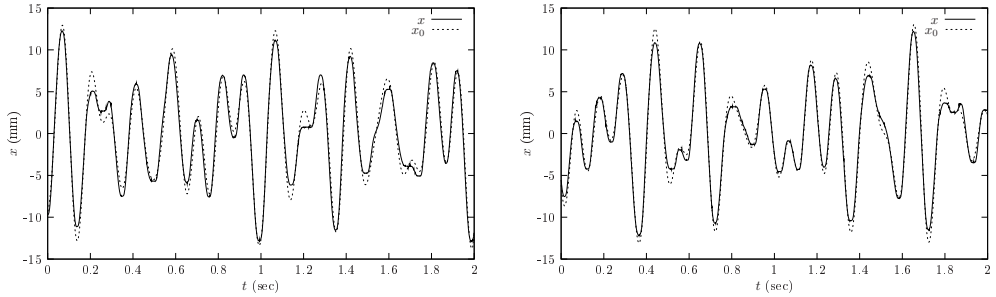

(a) $c = 1$ (b) $c = 15$

Fig. 9. Multi-sine tests. The reference signal is a weighted sum of sinusoids at $3, 4, 5, 6, 8, 9$&10Hz with amplitude adjusted to give displacements within the range of the equipment.

List of Tables

c	θ_m°
15	17.3
3	3.5
1	1.1

Table 1
Nominal phase-margin: $c = 15, 3, 1$

Parameter	Value
c_t	$191\text{Nm}^{-1}\text{s}$
k_t	36878Nm^{-1}
m_t	2.2kg

Table 2
Estimated transfer system parameters

c	c_e	θ_m°	g_m
15	1.00	96.6	1.42
15	0.50	25.0	1.51
15	0.20	19.7	1.77
15	0.01	17.9	2.31
3	1.00	9.6	1.08
3	0.50	5.0	1.10
3	0.20	3.7	1.15
3	0.01	3.7	1.26
1	1.00	3.1	1.03
1	0.50	1.8	1.04
1	0.20	1.1	1.06
1	0.01	1.1	1.09

Table 3
Phase and Gain margin